Hindawi
Shock and Vibration
Volume 2023, Article ID 9326195, 11 pages
https://doi.org/10.1155/2023/9326195

Research Article

Finite Element Model Updating of Steel Arch Bridge Based on First-Order Mode Test Data

Shuai Luo, Yingming Zhang, Jibao Shen, and Zhike Li

School of Civil Engineering, Shaoxing University, Shaoxing, Zhejiang 312000, China

Correspondence should be addressed to Shuai Luo; 839335743@qq.com

Received 26 October 2022; Revised 26 February 2023; Accepted 3 April 2023; Published 15 April 2023

Academic Editor: Fehmi Najar

Copyright © 2023 Shuai Luo et al. This is an open access article distributed under the Creative Commons Attribution License, which permits unrestricted use, distribution, and reproduction in any medium, provided the original work is properly cited.

In order to obtain an accurate finite element model of a steel arch bridge, a first-order modal finite element model updating method is proposed by using the measured first-order modal data of the bridge. Using the measured acceleration time history data under random excitation and the first-order mode updating method, the stiffness matrix of the finite element model is updated, and the first-order frequencies and first-order mode shapes before and after updating of the model are compared and analyzed. The state space method is used to compare and analyze the dynamic response and the reliability of the structure before and after the updating of the model. The results show that the difference of the first-order frequencies between the updated finite element model and the measured result is about 0.001, and the difference of the first-order mode shapes is less than 0.197, which meets the needs of engineering. Dynamic response values of the updated structural model are much larger than those of the structural model before updating. The theoretical model is different from the dynamic response of actual structure, so it is necessary to update the theoretical model. The finite element model updating method can provide a reliable analytical way for bridge structural health monitoring, state evaluation, and damage identification.

1. Introduction

Modern structural analysis generally depends on finite element models to predict dynamic behavior and understand the current state of a system [1]. The finite element theoretical model is established according to the parameters of the design drawing. There are some errors in the process of the structural design, which makes the initial finite element model deviate from the actual model [1, 2]. In addition, there are uncertainties in structural design parameters and some errors in the modeling process, so the finite element model needs to be modified according to the static test or dynamic test [3, 4]. The structure is subject to external erosion, fatigue load, and other adverse factors. With the passage of time, these adverse factors threaten the safety of the structure. A reasonable finite element model can truly reflect the state of the structure and predict the damage degree of the structure in advance, which can be used as a reliable basis for structural health monitoring and state evaluation [5–14].

Many researchers have done a lot of studies on the finite element updating method. Song and Weng considered that the structure has more overall degrees of freedom and more elements, in order to improve the efficiency of finite element model updating, the finite element model updating method of substructure is adopted, which only needs to calculate a small number of low-order modes of each substructure to reduce the model calculation time [15, 16]. Qin et al. combined Kriging agent model and improved particle swarm optimization algorithm and used structural load test data to modify the initial finite element model. Compared with the basic particle swarm optimization algorithm, the relative error is smaller and the modified model is more accurate [17]. Baisthakur and Chakraborty established a finite element model updating algorithm based on Monte Carlo under the Bayesian framework. Through the comprehensive test and measured data of the finite element model of a steel truss bridge, the effectiveness of the method is verified. Finally, the results of the algorithm are compared with the standard Monte Carlo algorithm, which shows that the algorithm is better than the standard Monte Carlo algorithm [18]. Wang et al. proposed a multiscale model updating method suitable for long-span cable-stayed bridges. This method suggests the overall and local structural response and carries out multiobjective optimization combined with the Kriging model. The updating results improve the accuracy of the multiscale model in the overall and local structural response [19]. Tran-Ngoc et al. measured the vibration of the South Australia railway bridge and updated the bridge model combined with particle swarm optimization algorithm and genetic algorithm. The accuracy of the algorithm is higher than that of a single algorithm and the cost is low [20]. Zhang proposed a model updating method based on free wave characteristics to pair the experimental mode and numerical prediction mode, so as to minimize the difference between the calculated free wave characteristics and the identified free baud. By comparing the measured frequency response function with the frequency response function obtained from the modified finite element model, the correctness of the calculation results is verified [18]. Zhao et al. proposed the BP neural network to modify the model, which can establish a more accurate finite element analysis model and make the modified result closer to the real stress state of the structure [21]. Yang et al. proposed a fast sensitivity analysis algorithm based on the reduced finite element model. The basic idea of the proposed sensitivity analysis algorithm is to use a model reduction technique to avoid the complex calculation required in solving eigenvalues and eigenvectors by the complete model [22].

Hence, there are still some problems in the model updating method, mainly due to the slow calculation speed and low accuracy [18]. Considering that the first-order modal information of the structure is easy to obtain, the first-order modal parameter identification result is more accurate and the identification speed is faster [21]. This study uses the acceleration time history data of steel arch bridge under random excitation to obtain the first-order frequency and first-order vibration mode. Combined with the first-order mode updating method, the model is updated to obtain the updated first-order frequency and first-order vibration mode, and the comparative analysis of the first-order mode before and after the bridge updating is carried out. In this paper, the dynamic responses of actual structure of the model before and after updating are obtained by using the state space theory.

2. Fundamental Theory

2.1. Updating Theory of First-Order Modal Finite Element Model. When the structure vibrates, the first modal characteristic equation of the n-DOF finite element model of the structure can be expressed as

$$K\Phi_1 = \lambda_1 M\Phi_1, \tag{1}$$

where K and M are the structural mass matrix and stiffness matrix of order $n \times n$, a $\lambda 1$ and Φ_1 are the first modal eigenvalues and corresponding eigenvectors, respectively, $\lambda 1$ is a number, and Φ_1 is the matrix of order $n \times 1$.

Let ΔK be the stiffness perturbation matrix reflecting the properties of the structure. The stiffness perturbation matrix is a sparse matrix, and its nonzero elements reflect the stiffness attenuation state. The first-order modal structural characteristic equation after structural stiffness attenuation can be expressed as

$$(K - \Delta K)\Phi_{1m} = \lambda_{1m} M\Phi_{1m}, \tag{2}$$

where ΔK is the perturbation stiffness matrix of order $n \times n$, λ_{1m} and Φ_{1m} are the first modal eigenvalues and corresponding eigenvectors obtained from the analysis of measured time history data, λ_{1m} is a number, and Φ_{1m} is the matrix of order $n \times 1$.

According to equation (2), the perturbation stiffness matrix can be expressed as

$$\Delta K = K - \lambda_{1m} M. \tag{3}$$

The residual R is defined as the product of the stiffness perturbation matrix and the measured vibration mode, which can be expressed as

$$R = \Delta K\Phi_{1m}, \tag{4}$$

where R is a column vector.

The stiffness matrix of attenuation can be also expressed as

$$\Delta K = \sum_i \alpha_i K, \tag{5}$$

where α_i is the attenuation coefficient of the element.

2.2. State Space Theory. The dynamic characteristics of the system need to be analyzed by using the state space theory [23–27]. In structural dynamics, the dynamics equation of a damped system with n degrees of freedom can be expressed as

$$M\ddot{u}(t) + C_0\dot{u}(t) + Ku(t) = U(t), \tag{6}$$

where M is the structural mass matrix, C_0 is the structural damping matrix, K is the structural stiffness matrix, $U(t)$ is the external load at time t, $\ddot{u}(t)$ is the acceleration response, $\dot{u}(t)$ is the velocity response, and $u(t)$ is the displacement response.

The output response is determined by the sampling frequency, and it has a certain time interval. Therefore, the output response should adopt the state space model of the discrete-time system. At the k sampling point, the discrete-time state space model of the system can be expressed as

$$\begin{aligned} X[k+1] &= \mathrm{AX}[k] + \mathrm{BU}[k], \\ Y[k] &= \mathrm{CX}[k] + \mathrm{DU}[k], \end{aligned} \tag{7}$$

where A is the state matrix of the discrete-time system, B is the input matrix of the discrete-time system, C is the observation matrix of the discrete-time system, and D is the input observation matrix.

2.3. Flow Chart of Model Updating. The finite element model of the steel arch bridge in this example is updated by the following process.

3. Engineering Example

3.1. Steel Arch Bridge Test. The project example is a steel cable bridge across the river, as shown in Figure 1. The structural form is an arch bridge, 18 cable pipelines are installed under the bottom beam, the cable model is YJV22-8.7/15, and the outer sleeve is a double wall corrugated pipe with a diameter of 160 mm. It was completed and put into use in 2007. The span of the steel arch bridge is 42 m, the arch height is 7.5 m, the bridge deck width is 3.5 m, and the suspender spacing is 4 m. The cross section of the bridge is shown in Figure 2. The lower beam is a box section, the sum width of the cover plate and bottom plate are 250 mm and 4 mm, respectively, and the sum width of web plate are 384 mm and 4 mm, respectively, as shown in Figure 3. There are 2.5 m steel jackets at both ends of the lower beam, and its section form is the box section. The length and width of the cover plate and bottom plate of the section are 290 mm and 8 mm, respectively, and the length and width of the web plate are 400 mm and 8 mm, respectively, as shown in Figure 4 The beam at the arch structure is a circular section with an outer diameter of 273 mm and a wall thickness of 6 mm. The middle suspender is an annular section with an outer diameter of 108 mm and a wall thickness of 3.5 mm. The deck checkered steel plate is 37 m long, 2.6 m wide, and 4 mm thick. The checkered steel plate is not welded to the lower beam. The transverse railing is mainly composed of one 76 mm diameter and two 50 mm diameter railings, each of which is 37 m long. There are 80 vertical railings with a diameter of 76 mm and a length of 1.1 m. The steel arch bridge is made of Q235 steel with a density of 7.85×10^3 kg/m^3 and elastic modulus is 200 GPa.

3.2. Acceleration Time History Measurement of Steel Arch Bridge. DH5907N dual channel acceleration sensor is used for field measurement. There are 5 collectors and 1 communication controller, as shown in Figure 5. The acceleration time history data of the lower beam at the lower node of the boom is measured by the sensor and synchronously transmitted to the computer through the wireless collector. As seen from Figure 6, there are 9 suspenders on one side of the bridge structure. Due to the limited number of sensors, sensors are arranged on the bridge twice for measurement. First of all, five sensors are placed at the suspender nodes 3, 4, 5, 6, and 7 on the left side of the mid-span, as shown in Figure 7(a). For the second time, place five sensors at the suspender nodes 7, 8, 9, 10, and 11 on the right side of the span, as shown in Figure 7(b). The excitation position is selected in the middle of the span. The measurement time of a group of data is about 3 minutes to obtain the measured data of bridge vibration.

3.3. Test Result. The acceleration time history data of the lower beam at the suspender node are measured, and the data of the attenuation section are intercepted to obtain the acceleration attenuation curve of the bridge after excitation. The acceleration attenuation curve of node 3 is shown in Figure 8. The first-order frequency can be obtained after Fourier transform [28] of the attenuation curve, as shown in Figure 9. It can be seen from the figure that the first-order frequency value is 3.369 Hz, the X coordinate value is the frequency value, and the Y coordinate is the amplitude corresponding to the frequency value.

Through the acceleration time history data measured by the acceleration sensor on the bridge deck, the first-order frequency value and the amplitude corresponding to the first-order frequency of each node are identified after Fourier transform. The vibration mode curve can be obtained by dividing the amplitude corresponding to the first-order frequency of each node by the maximum value of the amplitude corresponding to the frequency in the node, as shown in Figure 10.

4. Model Updating

4.1. Model Establishment. The steel arch bridge structure in this paper belongs to a relatively complex bridge structure system. The finite element model is established through the design drawings and relevant specifications. The finite element model diagram is shown in Figure 11. Steel arch bridge is regarded as a composite structure, and its stiffness matrix, mass matrix, and boundary conditions need to be treated to simplify the model and minimize the error of the model.

(1) *The Selection of Elements and the Establishment of Stiffness Matrix and Mass Matrix.* The internal force borne by the upper arch of the structure is axial force, shear force, and bending moment, so it is regarded as a beam element. Moreover, the arch structure is treated with a straight beam instead of a curved beam. The main beam at the lower part of the structure is treated as a beam element. The suspender is regarded as axial force link element, and the stiffness matrix and mass matrix of the structure are established. When establishing the stiffness and mass matrix of the lower beam, the influence of the stiffness and mass of bridge deck components such as railings and bridge decks on the stiffness and quality of the lower beam of the bridge is considered. The railing, deck slab, and other deck members increase the stiffness of the lower beam, so the corresponding vertical displacement element in the 37 m lower beam stiffness matrix needs to be multiplied by the additional stiffness coefficient of 2.2. Furthermore, the quality of railing, bridge deck, and other components will affect the vibration characteristics of the bridge. Therefore, the corresponding vertical displacement elements in the 37 m lower beam mass matrix need to be multiplied by the additional mass coefficient. The additional mass coefficient is as follows: the mass per meter of a main beam 42 m (excluding steel sleeve) is 43.96 kg, the total mass of the half bridge deck (37 m) structure (including guardrail and cable) is 132.1 kg per meter, and the

Figure 1: Bridge panorama.

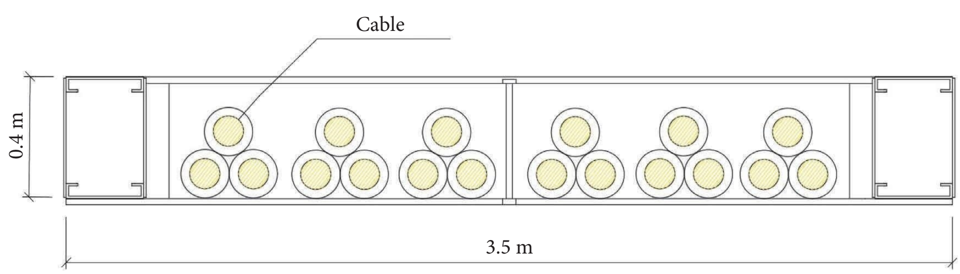

Figure 2: Cross section of bridge.

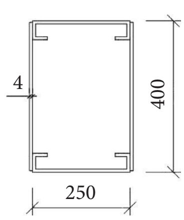

Figure 3: Bottom beam section.

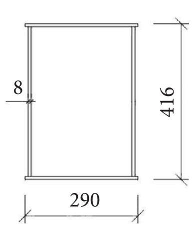

Figure 4: Steel jacket section.

additional coefficient of mass matrix is the total mass of structure per meter divided by the mass per meter of main beam, which is 3.0.

(2) *Determination of Boundary Conditions*. The steel arch bridge in this example adopts the concrete pouring method for the arch foot and lower main beam end of the main arch, and the boundary condition is fixed end constraint, which restricts the vertical displacement, horizontal displacement, and corner displacement of the arch foot and lower main beam end of the main arch.

The bar element stiffness matrix in the structure can be expressed as

$$K_e = \frac{EA}{L}\begin{bmatrix} 1 & -1 \\ -1 & 1 \end{bmatrix}, \tag{8}$$

where L is the length of the rod element, E is the elastic modulus, and A is the cross-sectional area.

The beam element stiffness matrix in the structure can be expressed as

(a) (b)

Figure 5: DH 5907N sensors: (a) communication controller and (b) collector.

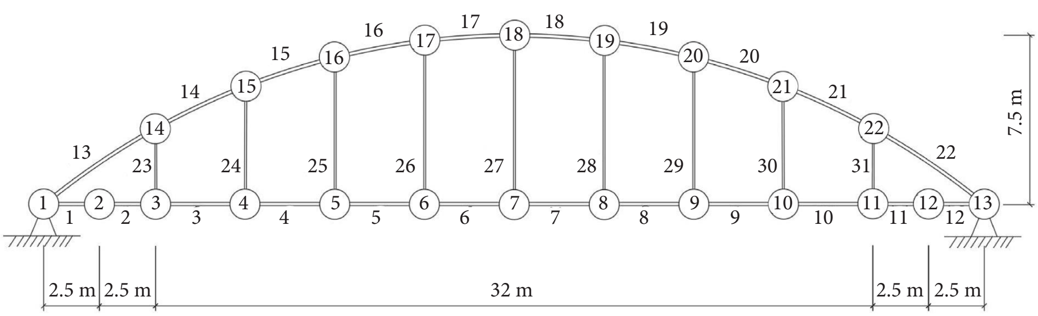

Figure 6: Model drawing of steel arch bridge.

$$K_f = \begin{bmatrix} \frac{EA_0}{L_0} & 0 & 0 & -\frac{EA_0}{L_0} & 0 & 0 \\ 0 & \frac{12EI}{L_0^3} & \frac{6EI}{L_0^2} & 0 & -\frac{12EI}{L_0^3} & \frac{6EI}{L_0^2} \\ 0 & \frac{6EI}{L_0^2} & \frac{4EI}{L_0} & 0 & -\frac{6EI}{L_0^2} & \frac{2EI}{L_0} \\ -\frac{EA_0}{L_0} & 0 & 0 & \frac{EA_0}{L_0} & 0 & 0 \\ 0 & -\frac{12EI}{L_0^3} & -\frac{6EI}{L_0^2} & 0 & \frac{12EI}{L_0^3} & -\frac{6EI}{L_0^2} \\ 0 & \frac{6EI}{L_0^2} & \frac{2EI}{L_0} & 0 & -\frac{6EI}{L_0^2} & \frac{4EI}{L_0} \end{bmatrix}, \tag{9}$$

where L_0 is the length of the rod unit and A_0 is the cross-sectional area.

The mass matrix of structural elements can be expressed as

$$M^e = \frac{\rho Al}{420} \begin{bmatrix} 140 & 0 & 0 & 70 & 0 & 0 \\ 0 & 156 & 22l & 0 & 54 & -13l \\ 0 & 22l & 4l^2 & 0 & 13l & -3l^2 \\ 70 & 0 & 0 & 140 & 0 & 0 \\ 0 & 54 & 13l & 0 & 156 & -22l \\ 0 & -13l & -3l^2 & 0 & -22l & 4l^2 \end{bmatrix}, \tag{10}$$

where ρ is the density, L is the unit length, and A is the cross-sectional area.

The transformation matrix T can be expressed as

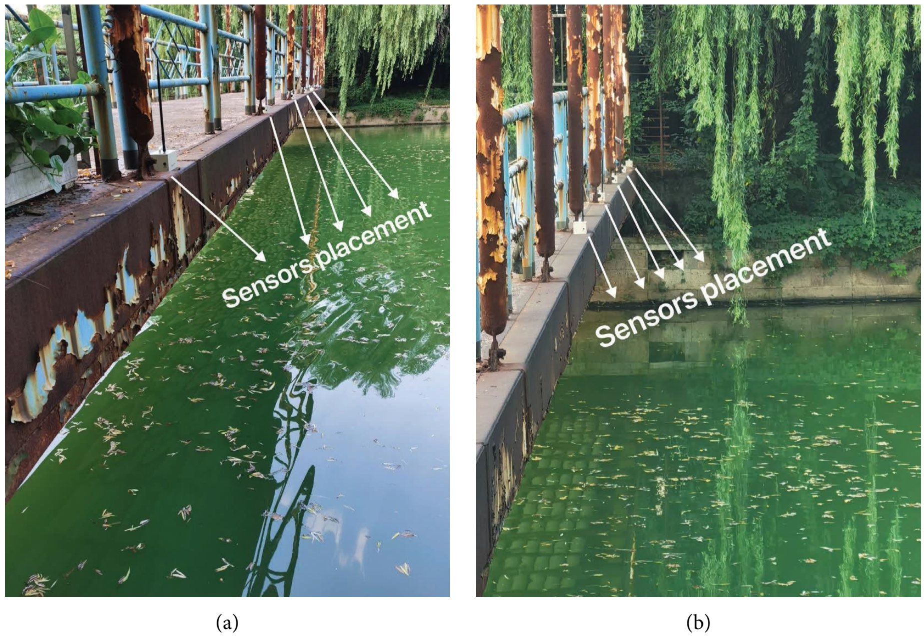

FIGURE 7: Measurement arrangement of sensors on-site: (a) arrangement on the left and (b) arrangement on the right.

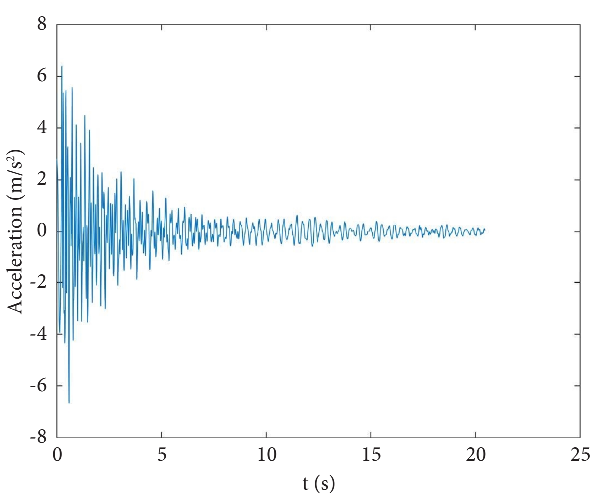

FIGURE 8: Acceleration decay time history curve.

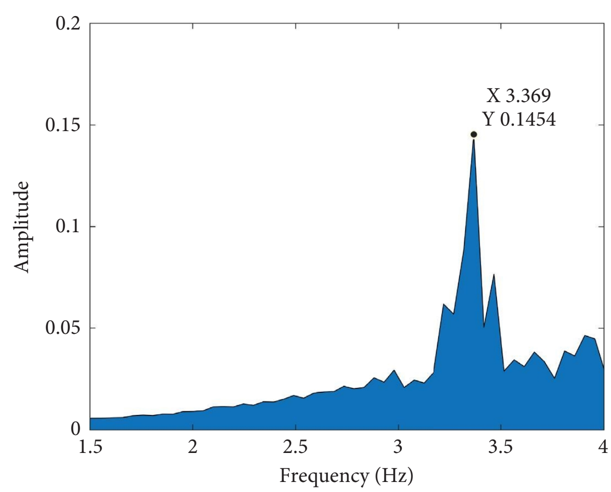

FIGURE 9: First-order frequency identification.

$$T = \begin{bmatrix} \cos\alpha & -\sin\alpha & 0 & 0 & 0 & 0 \\ \sin\alpha & \cos\alpha & 0 & 0 & 0 & 0 \\ 0 & 0 & 1 & 0 & 0 & 0 \\ 0 & 0 & 0 & \cos\alpha & -\sin\alpha & 0 \\ 0 & 0 & 0 & \sin\alpha & \cos\alpha & 0 \\ 0 & 0 & 0 & 0 & 0 & 1 \end{bmatrix}, \quad (11)$$

where α is the angle between the local coordinate system and the global coordinate system.

The element stiffness matrix K_e and element mass matrix M_e in the local coordinate system are transformed into the element stiffness matrix and mass matrix in the global coordinate system by the transformation matrix T. The element stiffness matrix and element mass matrix in the overall coordinate system are integrated by using the correlation table method [29] to obtain the overall stiffness matrix K_g and the overall mass matrix M_g.

Considering that the overall stiffness matrix of the structure needs to be updated, the updated stiffness matrix can be expressed as

$$K_{\mathrm{m}} = K_{\mathrm{g}} - \sum_i \alpha_i K_i^{\,g}, \quad (12)$$

where α_i is the attenuation coefficient and I is the unit number to be updated.

4.2. Model Updating and Updating Results. When the element stiffness matrix is updated, the damage degree of the

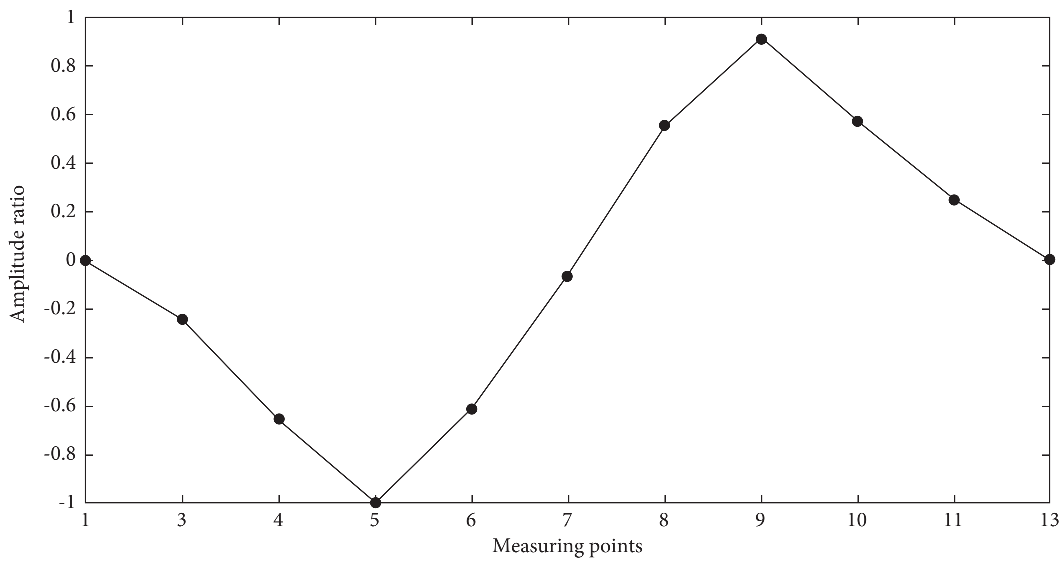

Figure 10: First-order mode vibration diagram.

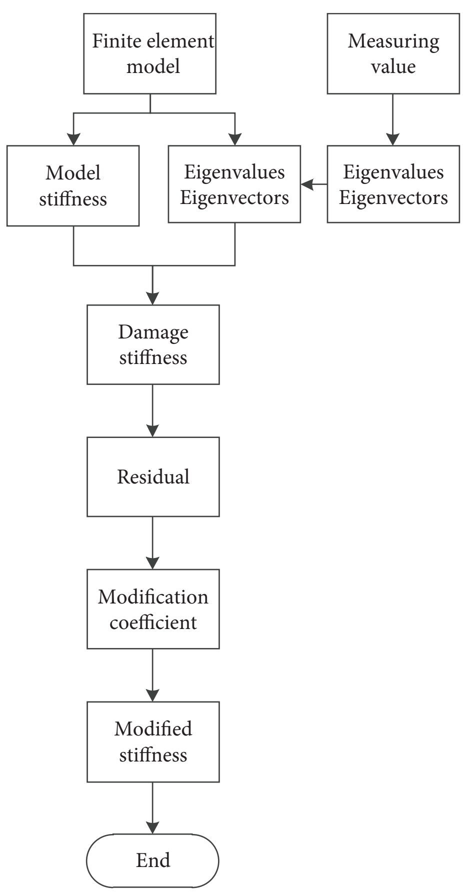

Figure 11: Updating process of finite element model.

actual upper main arch structure and suspender is small, mainly the damage degree of the lower beam is more serious. In this example, the stiffness matrix of the beam element with serious damage at the lower part is updated. Firstly, the overall stiffness matrix K_g and the overall mass matrix M_g are obtained through the integration of the element stiffness matrix. Secondly, analyze the measured acceleration time history data to obtain the first-order frequency and first-order vibration mode of bridge vibration. Replace the first-order frequency and first-order vibration mode into equation (2) to obtain the overall stiffness matrix to be updated. Finally, replace the overall stiffness matrix to be updated into equation (12) to calculate the stiffness attenuation coefficient of the corresponding stiffness attenuation element α_i. The stiffness of the arch bridge is calculated by software MATLAB. The attenuation coefficient of the arch bridge is calculated by the stiffness of the arch bridge α_i is 0.100, 0.101, 0.678, 0.259, 0.331, 0.207, 0.086, and 0.101, respectively.

After the element stiffness is updated by the first-order modal finite element algorithm, the updated stiffness matrix and mass matrix are substituted into formula (1), and the first-order modal frequency and first-order modal shape are obtained by MATLAB software. The first-order frequency values before and after updating and the difference between them and the test value are shown in Table 1. The first-order modal shape values of each node before and after updating and the difference between them and the measuring value are shown in Table 2.

Draw the measured vibration mode values in Table 2, the vibration mode values before updating and the updated vibration mode values, and obtain the test values, and the first-order vibration mode diagrams before and after updating, as shown in Figure 12.

The updating results in Tables 1 and 2 show that the first-order frequency difference of the steel arch bridge before updating is 0.427 Hz, and the first-order vibration mode difference is less than 0.306. After the first-order modal finite element updating method, the first-order frequency difference of the updating result is 0.001 Hz, and the first-order mode difference is less than 0.197 Hz. When using the first-order mode updating theory for updating calculation, the software has the reason of accuracy, so that the updated

Table 1: Comparison of first-order frequencies of before and after updating with the measuring value.

Measuring value	Before updating		After updating	
Frequency (Hz)	Frequency (Hz)	Difference (Hz)	Frequency (Hz)	Difference (Hz)
3.369	3.796	0.427	3.368	0.001

Table 2: Comparison of first-order mode shapes of before and after updating with the measuring value.

Measuring points	Measuring value	Before updating		After updating	
	Vibration mode	Vibration mode	Difference	Vibration mode	Difference
3	−0.243	−0.421	0.178	−0.340	0.097
4	−0.654	−0.877	0.223	−0.766	0.112
5	−1.000	−1.000	0.000	−1.000	0.000
6	−0.608	−0.660	0.052	−0.696	0.088
7	−0.065	0.000	0.065	0.016	0.081
8	0.553	0.660	0.107	0.650	0.097
9	0.917	1.000	0.083	0.918	0.001
10	0.571	0.877	0.306	0.768	0.197
11	0.247	0.421	0.174	0.357	0.110

Note. The vibration mode has been normalized. Nodes 1 and 13 are fixed ends, and their vibration mode value is 0, which is not listed in Table 2.

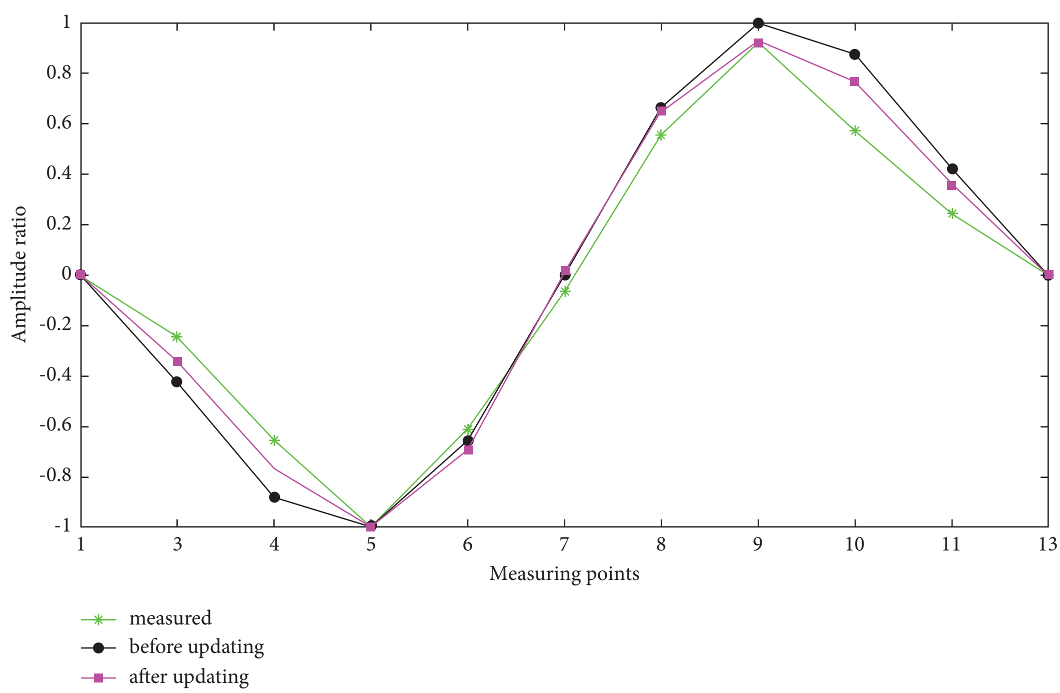

Figure 12: Comparison diagram of first-order mode shapes of before and after updating with measuring values.

value obtained by measuring point 6 and measuring point 7 is greater than the value before updating. To sum up, the updated difference is significantly smaller than that before updating. Moreover, the updated difference meets the requirements of practical engineering. Figure 12 shows that the updated first-order mode shape curve is closer to the measured first-order mode shape curve as a whole.

5. Dynamic Response Analysis

Dynamic analysis is the dynamic characteristic of structures subjected to random excitation. Using the state space theory in Section 2.2 to compare the dynamic analysis of the steel arch bridge model before and after updating, we can get the results of structural dynamic analysis before and after updating, and assess the degree of the structural damage under random excitation and how safe it is. The parameter setting value of this example is the sampling frequency $F_S = 100\,\text{Hz}$, the sampling interval $\triangle t = 1/F_s = 0.01\,\text{s}$, the number of samples generated $N = 5000$, and the damping matrix adopts the Rayleigh damping matrix [30]. Figure 13 shows the random excitation applied to the bridge. Figures 14 and 15 show the dynamic responses of displacement, velocity, and acceleration outputs before and after model

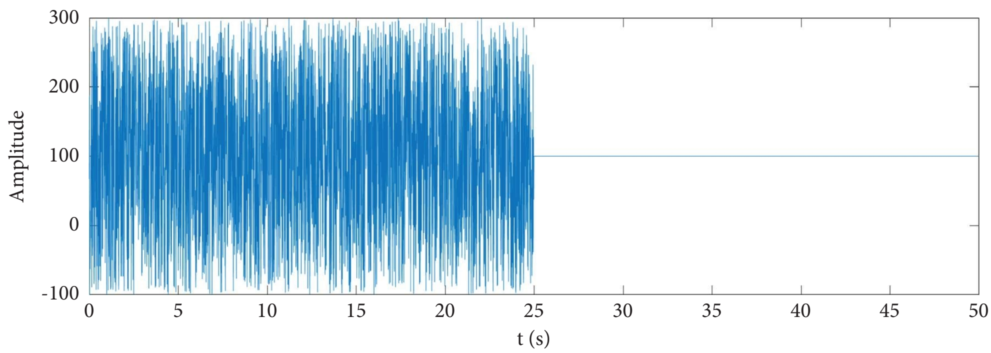

FIGURE 13: Random excitation signal.

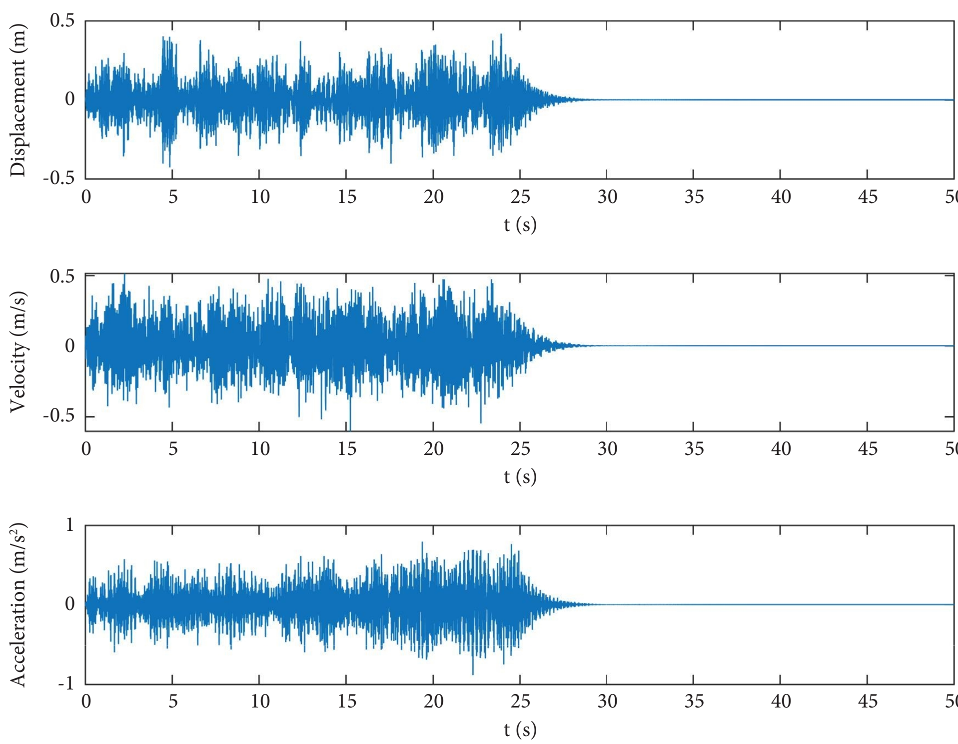

FIGURE 14: Dynamic responses output before update.

updating, respectively, and the peak value of the dynamic response in Figures 14 and 15 is the maximum value of displacement, velocity, and acceleration output dynamic response.

We extract the maximum dynamic analysis values of displacement, velocity, and acceleration before and after updating in Figures 14 and 15 and calculate the relative difference of dynamic analysis values of displacement, velocity, and acceleration before and after updating.

From Table 3, it can be seen that under the selected random excitation, the dynamic displacement response peak obtained by the bridge theoretical model is 0.421 m, reaching 1% of the bridge span. Under the same excitation, the peak displacement response, velocity response, and acceleration response of the modified model exceed the peak displacement response of the theoretical model by 20.7%, 32.1%, and 30.3%, respectively. With the increase of the bridge structure life and the environmental impact, the bridge stiffness will inevitably decrease, and among bridges, the dynamic response analysis differ significantly by different stiffness. Hence, it is necessary to modify the theoretical model. The updated model can prevent the bridge from the potential

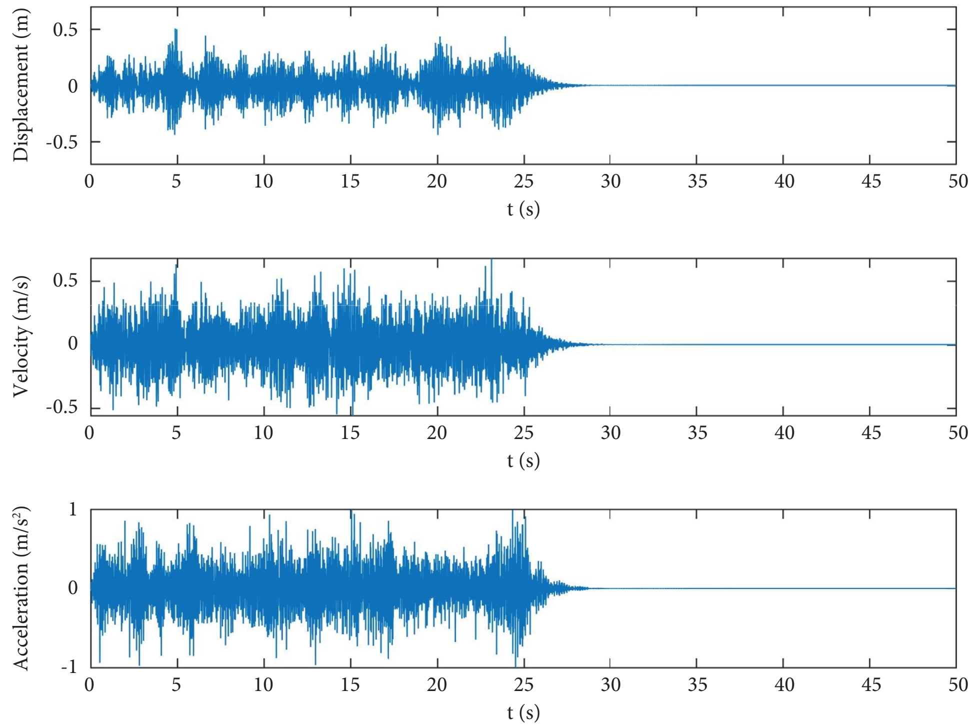

FIGURE 15: Dynamic responses output after update.

TABLE 3: Maximum dynamic response before and after updating the model.

Dynamic response	Before updating	After updating	Relative difference (%)
Displacement (m)	0.421	0.508	20.7
Speed (m/s)	0.516	0.682	32.1
Acceleration (m/s^2)	0.794	1.035	30.3

safety hazard of excessive peak dynamic response caused by severe environment such as typhoon and earthquake.

6. Conclusion

This study takes the actual steel arch bridge as the test object, uses the measured data of acceleration sensor for modal parameter analysis, uses the first-order modal updating method to modify the finite element model, compares and analyzes the first-order frequency and first-order vibration mode of the model before and after updating, and makes dynamic response analysis of the model before and after updating, and obtains the following conclusions:

(1) The first-order mode updating method is the finite element updating method. The updated first-order frequency difference is 0.001 Hz, and the updated first-order mode difference is within 0.197 Hz. The updating results meet the actual needs of the project.

(2) Under random excitation, the peak dynamic response of the structure before and after model modification is obtained by using the state space method. The dynamic response peaks of displacement, velocity, and acceleration after updating are much larger than those before updating. Therefore, after the theoretical model is modified, the dynamic characteristics of the structure under environmental dynamic excitation such as typhoon and earthquake can be obtained. Avoid potential safety hazards caused by excessive peak dynamic response of the structure.

(3) The updating results obtained by the first-order mode updating method can accurately reflect the dynamic characteristics of the structure, and this method has the advantages of simplicity and fast calculation speed. The updating results are close to the actual situation, which can provide an effective means for the actual structural health monitoring.

Data Availability

The data used to support the findings of this study are included within the article/supplementary material.

Conflicts of Interest

The authors declare that they have no conflicts of interest.

Supplementary Materials

The file “data” is the acceleration monitored by sensors. The file “wuxian” is the program of data analysis in our research group. The file “bMassMatrice2” is the mass matrix. The file “aStiffnessMatrice2truss” is the stiffness matrix. The file “updating” is the main work of our research group. (*Supplementary Materials*)

References

[1] D. T. Bartilson, J. Jang, and A. W. Smyth, “Finite element model updating using objective-consistent sensitivity-based parameter clustering and Bayesian regularization,” *Mechanical Systems and Signal Processing*, vol. 114, pp. 328–345, 2019.

[2] A. A. Mosavi, H. Sedarat, S. M. O’Connor, A. Emami-Naeini, and J. Lynch, “Calibrating a high-fidelity finite element model of a highway bridge using a multi-variable sensitivity-based optimisation approach,” *Structure and Infrastructure Engineering*, vol. 10, no. 5, pp. 627–642, 2014.

[3] G. Liu, J. Luo, Q. I. N. Yang, and J. Zhang, “A finite element model updating method based on improved MCMC method,” *Engineering Mechanics*, vol. 33, no. 6, 2016.

[4] J. Malveiro, D. Ribeiro, C. Sousa, and R. Calçada, “Model updating of a dynamic model of a composite steel-concrete railway viaduct based on experimental tests,” *Engineering Structures*, vol. 164, pp. 40–52, 2018.

[5] O. W. Petersen and O. Øiseth, “Sensitivity-based finite element model updating of a pontoon bridge,” *Engineering Structures*, vol. 150, pp. 573–584, 2017.

[6] E. Simoen, G. De Roeck, and G. Lombaert, “Dealing with uncertainty in model updating for damage assessment: a review,” *Mechanical Systems and Signal Processing*, vol. 56-57, pp. 123–149, 2015.

[7] S. Qin, Y. Zhou, H. Cao, and M. A. Wahab, “Model updating in complex bridge structures using kriging model ensemble with genetic algorithm,” *KSCE Journal of Civil Engineering*, vol. 22, no. 9, pp. 3567–3578, 2018.

[8] M. Pedram, A. Esfandiari, and M. R. Khedmati, “Finite element model updating using strain-based power spectral density for damage detection,” *Structural Control and Health Monitoring*, vol. 23, no. 11, pp. 1314–1333, 2016.

[9] W. Tian, S. Weng, Q. Xia, and Y. Xia, “Dynamic condensation approach for response-based finite element model updating of large-scale structures,” *Journal of Sound and Vibration*, vol. 506, Article ID 116176, 2021.

[10] B. Asgari, S. A. Osman, and A. Adnan, “Sensitivity analysis of the influence of structural parameters on dynamic behaviour of highly redundant cable-stayed bridges,” *Advances in Civil Engineering*, vol. 2013, Article ID 426932, 11 pages, 2013.

[11] L. Dai, “Finite-element model updating of the traditional beam–column joint in Tibetan heritage buildings using uniform design,” *Advances in Structural Engineering*, vol. 23, no. 9, pp. 1890–1901, 2020.

[12] S. Weng, H. Zhu, Y. Xia, J. Li, and W. Tian, “A review on dynamic substructuring methods for model updating and damage detection of large-scale structures,” *Advances in Structural Engineering*, vol. 23, no. 3, pp. 584–600, 2020.

[13] R. Hou and Y. Xia, “Review on the new development of vibration-based damage identification for civil engineering structures: 2010–2019,” *Journal of Sound and Vibration*, vol. 491, Article ID 115741, 2021.

[14] X. Peng and Q. Yang, “Damage detection in beam-like structures using static shear energy redistribution,” *Frontiers of Structural and Civil Engineering*, vol. 16, no. 12, pp. 1552–1564, 2023.

[15] X. Song, Y. Yan, J. Li, S. Weng, and S. Qin, “Substructure-based finite element model updating of long-span bridge,” *Bridge Construction*, vol. 22, 2021.

[16] S. Weng, Y. Xia, Y. L. Xu, and H. P. Zhu, “Substructure based approach to finite element model updating,” *Computers & Structures*, vol. 89, no. 9-10, pp. 772–782, 2011.

[17] S. Qin, J. Hu, H. Cao, J. Kang, and Q. Pu, “Finite element model updating of large-span arch bridge based on experimental data,” *China Journal of Highway and Transport*, vol. 32, no. 7, 2019.

[18] S. Baisthakur and A. Chakraborty, “Modified Hamiltonian Monte Carlo-based Bayesian finite element model updating of steel truss bridge,” *Structural Control and Health Monitoring*, vol. 27, no. 8, 2020.

[19] F. Y. Wang, Y. L. Xu, B. Sun, and Q. Zhu, “Updating multiscale model of a long-span cable-stayed bridge,” *Journal of Bridge Engineering*, vol. 23, no. 3, 2018.

[20] H. Tran-Ngoc, S. Khatir, G. De Roeck, T. Bui-Tien, L. Nguyen-Ngoc, and M. Abdel Wahab, “Model updating for nam O bridge using particle swarm optimization algorithm and genetic algorithm,” *Sensors*, vol. 18, no. 12, p. 4131, 2018.

[21] R. Zhao, Y. Wu, and Z. Feng, “Research for pedestrian steel bridge design of neural network in structural model updating,” *Shock and Vibration*, vol. 2022, Article ID 1057422, 11 pages, 2022.

[22] Q. Yang and X. Peng, “Sensitivity analysis using a reduced finite element model for structural damage identification,” *Materials*, vol. 14, no. 19, p. 5514, 2021.

[23] S. Luo, Z. Zhuang, W. Wang, and P. Jiang, “Residual mode vector-based structural damage identification with first-order modal information,” *Advances in Materials Science and Engineering*, vol. 2021, Article ID 5526171, 10 pages, 2021.

[24] T. Emmert, M. Meindl, S. Jaensch, and W. Polifke, “Linear state space interconnect modeling of acoustic systems,” *Acta Acustica United with Acustica*, vol. 102, no. 5, pp. 824–833, 2016.

[25] C. F. Silva, P. Pettersson, G. Iaccarino, and M. Ihme, “Uncertainty quantification of combustion noise by generalized polynomial chaos and state-space models,” *Combustion and Flame*, vol. 217, pp. 113–130, 2020.

[26] S. K. Varanasi and P. Jampana, “Nuclear norm subspace identification of continuous time state–space models with missing outputs,” *Control Engineering Practice*, vol. 95, Article ID 104239, 2020.

[27] S. Rangapuram, S. Matthias, G. Jan, S. Lorenzo, Y. Wang, and T. Januschowski, “Deep state space models for time series forecasting,” *Advances in Neural Information Processing Systems*, vol. 31, 2018.

[28] J. Leng, *Fourier Transform*, Tsinghua University Press, Tsinghua, China, 2004.

[29] H. Yang, S. Luo, G. Xing, and W. Wang, “Finite element analysis of bar and beam composite structure,” *Engineering Mechanics*, vol. 36, no. 1, 2019.

[30] S. Luo, J. Shen, Z. Li, and W. Wang, “A structural damage identification method based on arrangement of static force residual vector,” *Global Journal of Researches in Engineering*, vol. 22, no. 1, 2022.